Letter Vol. 50, No. 21/1 November 2025/Optics Letters 6618

Generalized Wigner–Smith theory for perturbations at resonant exceptional and diabolic point degeneracies

KAIYUAN WANG,[1,2] NIALL BYRNES,[1] AND MATTHEW R. FOREMAN[1,2,*]

[1]School of Electrical and Electronic Engineering, Nanyang Technological University, 50 Nanyang Avenue, Singapore 639798, Singapore
[2]Institute for Digital Molecular Analytics and Science, 59 Nanyang Drive, Singapore 636921, Singapore
*matthew.foreman@ntu.edu.sg

Received 7 August 2025; revised 9 September 2025; accepted 22 September 2025; posted 23 September 2025; published 23 October 2025

Resonant spectral degeneracies, including diabolic (DP) and exceptional (EP) points, exhibit unique sensitivity to external perturbations, enabling powerful control and engineering of wave phenomena. We present a residue-based perturbation theory that quantifies complex resonance splitting of DP and EP type spectral degeneracies using generalized Wigner–Smith operators. We validate our theory using both analytic Hamiltonian models and numerical electromagnetic simulations, demonstrating excellent agreement across a range of cases. Our approach accurately predicts degenerate resonance splitting using only scattering data, offering a powerful framework for sensitivity analysis, inverse design, and quantitative sensing. © 2025 Optica Publishing Group under the terms of the Optica Open Access Publishing Agreement.

https://doi.org/10.1364/OL.575813

The Wigner–Smith (WS) time delay operator, initially introduced in quantum scattering theory [1,2], serves as a fundamental tool for characterizing the temporal response of resonant systems. For a system described by a scattering matrix $\mathbf{S}(\omega)$, the real part of the eigenvalues of the WS matrix $\mathbf{Q}_\omega = -i\mathbf{S}^{-1}\,\partial_\omega \mathbf{S}$ quantifies the group delays of a set of incident wavepackets with modal structures given by the corresponding eigenvectors [3]. $\mathbf{Q}_\omega$ connects a system's frequency-domain response to its energetic and temporal properties, allowing studies of, e.g., time-delay statistics in chaotic cavities [4], light storage in random media [5], and density of states enhancement in nuclear physics [6]. More recently, generalized WS (GWS) operators of the form $\mathbf{Q}_\xi = -i\mathbf{S}^{-1}\partial_\xi \mathbf{S}$, where ξ denotes an arbitrary system parameter, have been proposed, extending conventional WS operators into parameter space and connecting external scattering observables to internal parametric sensitivities [7]. A key feature of GWS operators is that their principal modes, defined in analogy to the dispersion-free principal modes derived from $\mathbf{Q}_\omega$ [8], have been shown to exhibit insensitivity to the variable conjugate to ξ [9]. This insight has led to a wealth of advances in wavefront shaping and control [10], including targeted focusing in complex media [11], guided light delivery in deformed optical fibers [12], manipulation of optical forces and trap stiffness in microparticle systems [13], tailored energy redistribution in time-varying systems [14], and the construction of optimal information states for scattering measurements [15].

Recent studies have extended GWS operators to describe parametric spectral shifts in non-Hermitian systems [16,17]. In particular, Byrnes and Foreman [16] demonstrated that a complex analytic treatment of the GWS operator yields compact perturbative formulae for shifts in isolated resonances or anti-resonances associated with the poles and zeros of $\mathbf{S}$. Their treatment, however, was restricted to non-degenerate resonances associated with *simple* poles of $\mathbf{S}$ and therefore fails at diabolic points (DPs), where multiple resonant modes share the same frequency [18], and exceptional points (EPs), where resonant modes degenerate in frequency also become linearly dependent [19]. These degeneracies are not only mathematically rich, but also practically relevant. For example, DPs underpin mode-splitting sensors [20], while EPs enable chiral mode control, topological transport, and enhanced sensitivity [21–23]. A GWS framework that rigorously handles degenerate resonances remains lacking. In this work, we address this gap by developing a residue-based formalism that extends earlier perturbative formulae to arbitrary-order DP and EP type degeneracies and naturally reduces to earlier results in the non-degenerate case. We validate our derived formula using both analytic Hamiltonian models and electromagnetic simulations, thereby demonstrating its applicability to nanophotonic structures.

GWS perturbation theory at degenerate poles. We begin by briefly reviewing the key concepts from non-Hermitian physics most relevant to our study. More information can be found in Supplement 1 and the literature [24]. Consider a physical system with a non-Hermitian $N \times N$ Hamiltonian matrix $\mathbf{H}(\alpha) \in \mathbb{C}^{N\times N}$ depending on a complex parameter α. Our work concerns *resonant* DP and EPs associated with the eigenmodes of $\mathbf{H}$, as opposed to *scattering* DP and EPs associated with those of $\mathbf{S}$ [25]. We assume that for a particular parameter value $\alpha = \alpha_0$, $\mathbf{H}(\alpha_0)$ has a repeated (degenerate) eigenvalue ω_p with algebraic multiplicity AM = N and geometric multiplicity GM satisfying $1 \le \mathrm{GM} \le N$. When AM = GM, $\mathbf{H}(\alpha_0)$ is diagonalizable and the degeneracy corresponds to a DP. When GM < AM, however, $\mathbf{H}(\alpha_0)$ is defective and contains at least one Jordan block of size greater than one. For our purposes, an EP will correspond to the case GM = 1, meaning $\mathbf{H}(\alpha_0)$ contains a sin-

gle Jordan block of size $N \times N$. Intermediate cases $1 < \mathrm{GM} < N$ correspond to hybrid DP-EP scenarios as discussed below.

Suppose first that the system possesses an EP and is perturbed so that α shifts from α_0 to a nearby value. We assume that this perturbation is generic, meaning the degeneracy is lifted and ω_p splits into N distinct eigenvalues ω_n $(n = 1, \ldots, N)$. At a point α in the neighborhood of α_0, the eigenfrequencies admit a Puiseux expansion [26]:

$$\omega_n(\alpha) = \omega_p + c\, e^{2\pi i n/N} \Delta\alpha^{1/N} + \mathcal{O}(\Delta\alpha^{2/N}), \tag{1}$$

where $\Delta\alpha = \alpha - \alpha_0$ and $c \in \mathbb{C} \neq 0$. We note immediately that Eq. (1) implies that, to leading order, the degenerate eigenvalue splits symmetrically and shifts in proportion to $\Delta\alpha^{1/N}$. Deviations from this scaling have been reported for systems experiencing non-generic perturbations, such as those preserving symmetry [27]. Such cases are beyond the scope of this work.

In addition to $\Delta\alpha$, the shift sensitivity is also governed by the coefficient c, which remains to be determined. It has been shown elsewhere that this coefficient is related to the orthogonality of the eigenvectors of $\mathbf{H}(\alpha_0)$ [28]. Here we show that it can also be related to the scattering matrix $\mathbf{S} \in \mathbb{C}^{M\times M}$. A commonly used expression for $\mathbf{S}$ in terms of $\mathbf{H}$ is given by [29]:

$$\mathbf{S}(\omega, \alpha) = \mathbf{I}_M - i\,\mathbf{W}^\dagger(\omega \mathbf{I}_N - \mathbf{H}(\alpha))^{-1}\mathbf{W}, \tag{2}$$

where $\mathbf{I}_M$ is the $M \times M$ identity matrix and $\mathbf{W} \in \mathbb{C}^{N\times M}$ couples the N internal modes of the system to M external scattering channels. A key property of Eq. (2) is that degenerate eigenfrequencies of $\mathbf{H}$ are mapped to degenerate poles of $\mathbf{S}$ via the resolvent $(\omega \mathbf{I}_N - \mathbf{H}(\alpha))^{-1}$. It has also been shown that [30]:

$$c^N = -\frac{\partial}{\partial\alpha} \det[\omega \mathbf{I}_N - \mathbf{H}(\alpha)]\Big|_{\omega=\omega_p,\ \alpha=\alpha_0}, \tag{3}$$

which can be linked to Eq. (2) using the identity:

$$\det[\omega \mathbf{I}_N - \mathbf{H}(\alpha)] = \det[\mathbf{S}^{-1}(\omega, \alpha)]\, g(\omega, \alpha), \tag{4}$$

where $g(\omega, \alpha) = \det[\omega \mathbf{I}_N - \mathbf{H}(\alpha) - i\mathbf{W}\mathbf{W}^\dagger]$. A short derivation of Eq. (4) is given in Supplement 1. Differentiating Eq. (4) with respect to α and applying Jacobi's identity to the derivative of $\det(\mathbf{S}^{-1})$, we can obtain c^N by evaluating the limit:

$$c^N = \lim_{\omega\to\omega_p} (\omega - \omega_p)^N \left(i\,\mathrm{tr}[\mathbf{Q}_\alpha(\omega, \alpha)] - \frac{1}{g}\frac{\partial g}{\partial\alpha} \right)\Big|_{\alpha=\alpha_0}, \tag{5}$$

where we have used $\det[\omega \mathbf{I}_N - \mathbf{H}(\alpha_0)] = (\omega - \omega_p)^N$. To proceed, we note that the final term in Eq. (5) vanishes provided that $\mathbf{W}$ is non-zero (see Supplement 1). Standard limit laws allow us to write $c = \mathrm{Res}_{\omega=\omega_p}\{[i\,\mathrm{tr}\,\mathbf{Q}_\alpha(\omega, \alpha_0)]^{1/N}\}$, which can be substituted back into Eq. (1). Neglecting higher order terms yields the resonance shift formula:

$$\Delta\omega_n = e^{2\pi i n/N}\, \Delta\alpha^{1/N}\, \mathrm{Res}_{\omega=\omega_p}\left\{[i\,\mathrm{tr}\,\mathbf{Q}_\alpha(\omega, \alpha_0)]^{1/N}\right\}, \tag{6}$$

where $\Delta\omega_n = \omega_n - \omega_p$. Notably, Eq. (6) exhibits the correct fractional power scaling and reduces to the non-degenerate pole shift formula when $N = 1$ [16,17]. Finally, it is easy to show by considering $\mathbf{S}^{-1}$ instead of $\mathbf{S}$, that our analysis equally applies to splitting of degenerate scattering zeros, e.g., at coherent perfectly absorbing EPs [31].

We now turn our attention to DPs, where $\mathrm{GM} = N$ and the Jordan normal form of $\mathbf{H}(\alpha_0)$ is diagonal with repeated entry ω_p. In contrast to EPs, where eigenvalue shifts are strongly correlated, the linear independence of modes at a DP allows the eigenvalues to shift independently, each admitting their own Taylor expansion. Consequently, Eq. (6) cannot recover all frequency shifts and an alternative approach is required. In principle, the N frequency shifts could be determined by constructing GWS operators from a suitable set of N scattering functions, each isolating a single pole associated with one of the DP modes. Application of the non-degenerate theory to each of these operators would then yield the N desired frequency shifts. The feasibility of this approach, however, depends intricately on the form of $\mathbf{W}$ and $\mathbf{H}$. $\mathbf{W}$ having full rank, particularly when $M \geq N$ (at least as many scattering channels as internal modes), ensures that $\mathbf{S}$ possesses N non-zero eigenvalues. These eigenvalues, which can easily be extracted from $\mathbf{S}$, are natural candidates for the desired set of scattering functions. In general, however, a single eigenvalue of $\mathbf{S}$ can depend on multiple eigenfrequencies of $\mathbf{H}$ and additional constraints are required to ensure that the poles are cleanly separated.

One simple class of $\mathbf{W}$ matrices for which the eigenvalues of $\mathbf{H}$ do not mix among those of $\mathbf{S}$ can be found by observing the algebraic structure of Eq. (2). Note first that although $\mathbf{W}$ is not in general square, it possess a right inverse $\mathbf{W}_R = \mathbf{W}^\dagger(\mathbf{W}\mathbf{W}^\dagger)^{-1}$. If $\mathbf{W}\mathbf{W}^\dagger = \gamma \mathbf{I}_N$ for some constant γ, then it follows that $\mathbf{W}^\dagger = \gamma \mathbf{W}_R$, and Eq. (2) thus expresses pseudo-similarity between $\mathbf{S}$ and $\mathbf{H}$. Physically, this condition dictates that each internal mode couples to the exterior through orthogonal, non-interfering channels with uniform coupling strength γ. The eigenvalues of $\mathbf{S}$ will then be of the form $\mu_n = 1 - i\gamma(\omega - \omega_n)^{-1}$ and analysis of the operators $Q_{\alpha,n} = -i\mu_n^{-1}\partial_\alpha \mu_n$ yields the pole shifts. Though this condition is sufficient to avoid mixing, it is not necessary, and pole mixing can be avoided even in cases where $\mathbf{W}\mathbf{W}^\dagger$ is not diagonal. An example of such a case is presented in Supplement 1, but an exhaustive analysis is beyond the scope of this paper. In any case, we note that if the form of $\mathbf{W}$ is known, one can always compute its inverse directly and obtain the resolvent $(\omega \mathbf{I}_N - \mathbf{H})^{-1} = -i\mathbf{W}_R^\dagger(\mathbf{S} - \mathbf{I}_M)\mathbf{W}_R$, whose eigenvalues each are of the form $(\omega - \omega_n)^{-1}$. This calculation reverts the problematic mixing caused by $\mathbf{W}$, yielding a set of functions that can be used to find the pole shifts. As a final remark, we note that the cases $1 < \mathrm{GM} < N$ present similar challenges associated with the structure of $\mathbf{W}$. In principle, however, the analysis can be restricted to each Jordan block individually, allowing the techniques described to be applied to each one.

EP and DP in a two-level system. To verify our theory, we now apply it to the analysis of perturbations to a canonical, non-Hermitian model widely used to describe coupled microring resonators and similar photonic dimers [32]. This system is characterized by the 2×2 effective Hamiltonian:

$$\mathbf{H}(\kappa) = \begin{pmatrix} \omega_1 - i\gamma_1/2 & \kappa \\ \kappa & \omega_2 - i\gamma_2/2 \end{pmatrix}, \tag{7}$$

where ω_1 and ω_2 are the resonant frequencies of the two modes, γ_1 and γ_2 represent their loss rates, and κ is the complex coupling amplitude. For convenience, the detuning and loss contrast are defined as $\Omega \equiv \omega_1 - \omega_2$ and $\Gamma \equiv \gamma_1 - \gamma_2$, respectively. An EP arises when $\kappa = \kappa_{\mathrm{EP}}$ is such that $\det[\omega \mathbf{I} - \mathbf{H}(\kappa_{\mathrm{EP}})] = 0$ has a repeated root $\omega = \omega_{\mathrm{EP}}$, which occurs when $\kappa_{\mathrm{EP}} = \pm i(\Omega/2 - i\Gamma/4)$ and $\omega_{\mathrm{EP}} = (\omega_1 + \omega_2)/2 - i(\gamma_1 + \gamma_2)/4$. For a small deviation $\kappa = \kappa_{\mathrm{EP}} + \delta\kappa$ with $|\delta\kappa| \ll |\kappa_{\mathrm{EP}}|$, direct diagonalization of the resulting $\mathbf{H}$ yields the leading-order eigen-splitting:

$$\Delta\omega_\pm \simeq \pm\sqrt{2\,\kappa_{\mathrm{EP}}\,\delta\kappa}. \tag{8}$$

To compare Eq. (8) to Eq. (6) for the dimer system, we must first define the form of the channel matrix $\mathbf{W}$. For simplicity, we choose $\mathbf{W} = \mathrm{diag}(\sqrt{\gamma_{1c}}, \sqrt{\gamma_{2c}})$, which couples each internal mode to an independent external channel with rates γ_{1c} and γ_{2c}. The introduction of $\mathbf{W}$ requires us to modify the effective Hamiltonian according to $\mathbf{H} \to \mathbf{H} - i\mathbf{W}\mathbf{W}^\dagger/2$, which, given the form of $\mathbf{W}$, is equivalent to redefining the loss rates in Eq. (7) according to $\gamma_i \to \gamma_i + \gamma_{ic}$. With these redefinitions, the forms of κ_{EP} and ω_{EP} as given above remain invariant. Using Eq. (2), the scattering matrix and corresponding GWS operator $\mathbf{Q}_\kappa$ can be computed. After some algebra, we find:

$$\operatorname*{Res}_{\omega=\omega_0} \left[\sqrt{i\,\mathrm{tr}\,\mathbf{Q}_\kappa(\kappa_{\mathrm{EP}})} \right] = \sqrt{2\kappa_{\mathrm{EP}}}, \tag{9}$$

which, when substituted into Eq. (6) with $N = 2$, yields $\Delta\omega_\pm = \pm\sqrt{2\,\kappa_{\mathrm{EP}}\,\delta\kappa}$, in exact agreement with Eq. (8).

By adjusting the parameters in Eq. (7), we can construct a DP within the same mathematical framework. This can be achieved by setting $\Omega = \Gamma = 0$, which reduces the effective Hamiltonain to $\mathbf{H} = (\omega_0 - i\gamma/2)\mathbf{I}_2 + \kappa\mathbf{J}_2$, where $\mathbf{J}_2$ is the 2×2 exchange matrix and $\omega_0 = \omega_1 (= \omega_2)$. This case now trivially admits a DP at $\kappa_{\mathrm{DP}} = 0$ with repeated eigenvalue $\omega_0 - i\gamma/2$. Altering κ by $\delta\kappa$ shifts the eigenvalues linearly by $\Delta\omega_\pm = \mp\delta\kappa$. At the same time, with $\mathbf{W}$ defined as before, but with $\gamma_{1c} = \gamma_{2c} = \gamma_c$ and $\gamma \to \gamma + \gamma_c$, it is straightforward to show that the eigenvalues of $\mathbf{S}$ are given by $\mu_\pm = 1 - i\gamma_c(\omega - \omega_0 + i\gamma/2 \pm \kappa)^{-1}$. Note that this form of $\mathbf{W}$ satisfies the property $\mathbf{W}\mathbf{W}^\dagger = \gamma\mathbf{I}_2$ as discussed above and does not result in pole mixing among $\mu_\pm$. The GWS operator $Q_{\kappa,\pm} = -i\mu_\pm^{-1}\partial_\kappa\mu_\pm$ is then given by:

$$Q_{\kappa,\pm} = \frac{\pm\gamma_c}{(\omega - \omega_0 + i\gamma/2 \pm \kappa)(\omega - \omega_0 + i\gamma/2 \pm \kappa - i\gamma_c)}, \tag{10}$$

which, after partial fraction decomposition, can be shown to have residue $\pm i$ at $\omega = \omega_0 - i\gamma/2$ when $\kappa = 0$. Equation (6) with $N = 1$ therefore predicts $\Delta\omega_\pm = \mp\delta\kappa$ as expected.

DP in ellipsoidal nanoparticles. We now consider the case of a DP in a small, homogeneous, metallic ellipsoid. Our ellipsoid, embedded in a background of unity permittivity, has semi-axes a_1, a_2, a_3 (see inset of Fig. 1) and complex permittivity $\varepsilon(\omega)$ taken as that of gold assuming a Drude–Lorentz model [33]. In a coordinate system aligned with the ellipsoid's principal axes, the 3×3 polarizability tensor is diagonal with entries [34]:

$$\mathcal{P}_i(\omega) \sim \frac{\varepsilon(\omega) - 1}{1 + L_i[\varepsilon(\omega) - 1]}, \tag{11}$$

where L_i are geometrical factors. In the case of a sphere ($a_1 = a_2 = a_3$), $L_1 = L_2 = L_3 = 1/3$ and the principal polarizabilities become degenerate, each exhibiting a pole ω_p at the Fröhlich resonance condition $\varepsilon(\omega_p) = -2$. The sphere therefore constitutes a DP in the space of ellipsoid shapes with the polarizability tensor playing the role of the scattering matrix.

A small axial perturbation to the j'th semi-axis of the sphere, $a_j \to a_j + \Delta a_j$, breaks the geometric symmetry, partially lifting the degeneracy. The pole shifts in each polarizibility component can be found by analyzing the functions $Q_{\Delta a_j,i} = -i\mathcal{P}_i^{-1}\partial_{\Delta a_j}\mathcal{P}_i$, from which we find that the pole in $\mathcal{P}_i$, $\omega_{p,i}$, shifts according to:

$$\Delta\omega_{p,i} = \Delta a_j \frac{6(1 - 3\delta_{ij})}{5a} \operatorname*{Res}_{\omega=\omega_p} \left(\frac{1}{\varepsilon(\omega) + 2} \right), \tag{12}$$

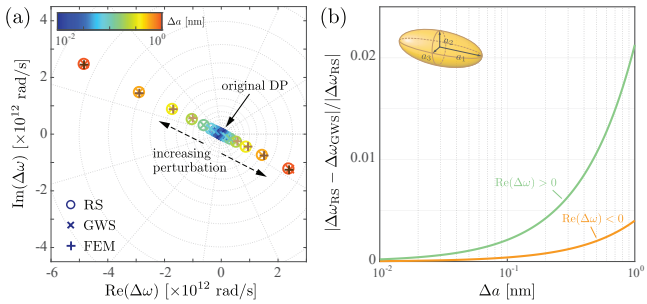

Fig. 1. (a) Trajectories of poles in the polarizability of an initially spherical nanoparticle subjected to an axial elongation (inset) along its first principal axis ($a_1 \to a_1 + \Delta a$) as computed by root searching (RS, ∘ markers), our GWS residue formula (× markers), and full FEM simulations (+ markers). Colors indicate perturbation amplitude Δa on a logarithmic scale. (b) Magnitude of the relative difference in pole shifts for both branches as obtained from the RS and GWS methods as a function of Δa.

where a is the sphere radius. Notably, Eq. (12) shows that the pole associated with the elongated axis shifts in the opposite direction to those of the other two axes, with twice the magnitude. The polarizabilities of the remaining axes stay degenerate, as their symmetry is preserved. To test the validity of Eq. (12), we compared it to the results of two additional methods: root-tracking of the inverse of the quasistatic polarizability, and numerical tracking of the poles using finite-element (FEM) simulations in COMSOL. In particular, we considered shifts in a degenerate localized surface plasmon resonance at $\omega_p \simeq (3700 - 400i) \times 10^{12}$ rad/s in a sphere of radius 50 nm, stretched along one axis with Δa ranging from 10^{-2} to 1 nm in 10 log-spaced intervals. Figure 1(a) compares the computed complex frequency shifts. As can be seen, all three methods show good quantitative agreement across the range of perturbations considered. The pole splitting is clearly visible, with the poles traversing two oppositely directed branches. The upper-left branch ($\mathrm{Re}(\Delta\omega) < 0$) corresponds to $i = j$ (the pole in the polarizability of the perturbed axis) and features points spaced twice as far apart as those on the doubly degenerate, lower-right branch ($\mathrm{Re}(\Delta\omega) > 0$), which corresponds to $i \neq j$ (poles in polarizabilities of the unperturbed axes). Figure 1(b) shows the relative numerical differences between the GWS and numerical root-based approaches, confirming the agreement seen in (a). Quadratic error growth found in both branches is consistent with the neglect of higher-order terms in Eq. (1).

EPs in plasmonic nanowires. As a final test of our theory, we investigate a class of plasmonic structures designed using transformation optics (TO) to support EPs of orders two, three, and four (denoted EP_2, EP_3, and EP_4, respectively) [35]. The corresponding compound nanowire and dimer structures are depicted schematically in the insets of Figs. 2(a)–2(c). We introduce a perturbation in the background dielectric permittivity, $\epsilon_h \to \epsilon_h + \Delta\epsilon(\mathbf{r})$, and again track the resulting shifts in the complex resonance frequencies. Resonance shifts are computed first by directly solving the perturbed dispersion relation of the TO-based system [35] and secondly by applying Eq. (6) with the system's transfer matrix, whose poles also capture the EP, used in place of $\mathbf{S}$. Residue-based predictions and numerically extracted root trajectories are shown in Figs. 2(a)–2(c) for each EP order. Good agreement between the GWS residue formula

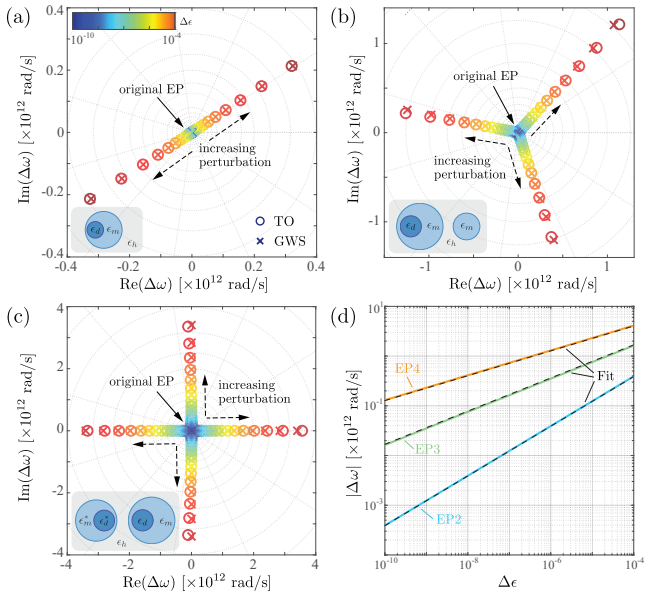

Fig. 2. Splitting in the complex plane of (a) EP_2, (b) EP_3, and (c) EP_4 degenerate resonances supported in TO-designed plasmonic nanowire structures (insets) upon a perturbation, $\Delta\varepsilon$, of the host permittivity. Complex frequency shifts were calculated from direct solution of the TO dispersion relation (∘ markers) and our GWS residue formula (× markers). Marker color encodes $\Delta\varepsilon$ on a logarithmic scale. (d) Log–log plot of the magnitude of the frequency shift $|\Delta\omega|$ versus $\Delta\varepsilon$ for each EP. Gradients of 1/2, 1/3, and 1/4 are found for EP_2, EP_3 and EP_4 respectively (black dashed fits).

(crosses) and the TO-based solutions (circles) over six orders of magnitude variation in $\Delta\varepsilon$ (as depicted by marker color) is evident. Each EP of order N also exhibits a N fold symmetric splitting as predicted by Eq. (6). Minor deviations arise at the largest perturbation amplitudes ($\Delta\varepsilon \sim 10^{-4}$), particularly for higher-order EPs, which likely arise due to neglecting higher order terms in the perturbative expansion as well as potentially inaccuracies from the TO-based approach, given the nanowire dimensions used. Plots of $|\Delta\omega|$ are also shown in Fig. 2(d) confirming the theoretical $\Delta\varepsilon^{1/N}$ scaling (note that identical plots are found for each branch).

In conclusion, we have developed a perturbative framework that extends prior GWS perturbation theory to non-Hermitian systems exhibiting EPs and DPs. Our approach shares the merits of previous iterations and enables determination of internal resonant behavior from external scattering measurements in a flexible and straightforward way [16,17]. Our theory was validated through analytic modelling and electromagnetic simulations of assorted nanophotonic and TO-engineered plasmonic systems. The final example in particular also demonstrates that although Eq. (6) was derived based on Eq. (2), it does not depend on this exact relation and can also be used in situations where neither **H** nor **S** are convenient to describe. Our results demonstrate the method's accuracy, generality, and computational practicality, offering new perspectives and tools for sensitivity analysis, quantitative sensing, resonance control and inverse design of complex non-Hermitian environments (see, e.g., [16,17]).

Funding. Ministry of Education – Singapore (RG66/23, EDUN C-33-18-279-V12); Nanyang Technological University (SUG:022824-00001, IGP-RSS).

Disclosures. The authors declare no conflicts of interest.

Data availability. Data may be obtained from the authors upon reasonable request.

Supplemental document. See Supplement 1 for supporting content.

REFERENCES

1. E. P. Wigner, Phys. Rev. **98**, 145 (1955).
2. F. T. Smith, Phys. Rev. **118**, 349 (1960).
3. U. R. Patel and E. Michielssen, IEEE Trans. Antennas Propag. **69**, 902 (2021).
4. A. Grabsch, D. V. Savin, and C. Texier, J. Phys. A: Math. Theor. **51**, 404001 (2018).
5. M. Durand, S. M. Popoff, R. Carminati, *et al.*, Phys. Rev. Lett. **123**, 243901 (2019).
6. M. D. Higgins, C. H. Greene, A. Kievsky, *et al.*, Phys. Rev. Lett. **125**, 052501 (2020).
7. M. Horodynski, M. Kühmayer, A. Brandstötter, *et al.*, Nat. Photonics **14**, 149 (2020).
8. J. Carpenter, B. J. Eggleton, and J. Schröder, Nat. Photonics **9**, 751 (2015).
9. P. Ambichl, A. Brandstötter, J. Böhm, *et al.*, Phys. Rev. Lett. **119**, 033903 (2017).
10. P. Del Hougne, K. B. Yeo, P. Besnier, *et al.*, Phys. Rev. Lett. **126**, 193903 (2021).
11. J. Sol, L. L. Magoarou, and P. del Hougne, Laser Photonics Rev. **19**, 2400619 (2025).
12. M. W. Matthès, Y. Bromberg, J. D. Rosny, *et al.*, Phys. Rev. X **11**, 021060 (2021).
13. U. G. Būtaitė, C. Sharp, M. Horodynski, *et al.*, Sci. Adv. **10**, eadi7792 (2024).
14. J. Hüpfl, N. Bachelard, M. Kaczvinszki, *et al.*, Phys. Rev. Lett. **130**, 083203 (2023).
15. D. Bouchet, S. Rotter, and A. P. Mosk, Nat. Phys. **17**, 564 (2021).
16. N. Byrnes and M. R. Foreman, Newton **1**, 100194 (2025).
17. N. Byrnes and M. R. Foreman, Phys. Rev. Res. **7**, 013299 (2025).
18. M. V. Berry and M. Wilkinson, Proc. Roy. Soc. London A. Math. Phys. Sci. **392**, 15 (1984).
19. M. A. Miri and A. Alu, Science **363**, eaar7709 (2019).
20. J. Zhu, S. K. Ozdemir, Y.-F. Xiao, *et al.*, Nat. Photonics **4**, 46 (2010).
21. Y.-H. Lai, Y.-K. Lu, M.-G. Suh, *et al.*, Nature **576**, 65 (2019).
22. Z. Li, C. Li, Z. Xiong, *et al.*, Phys. Rev. Lett. **130**, 227201 (2023).
23. H. Loughlin and V. Sudhir, Phys. Rev. Lett. **132**, 243601 (2024).
24. Y. Ashida, Z. Gong, and M. Ueda, Adv. Phys. **69**, 249 (2020).
25. W. R. Sweeney, C. W. Hsu, S. Rotter, *et al.*, Phys. Rev. Lett. **122**, 093901 (2019).
26. T. Kato, *Perturbation Theory for Linear Operators*, Vol. **132** of Classics in Mathematics (Springer Science & Business Media, 2013).
27. D. Grom, J. Kullig, M. Röntgen, *et al.*, Phys. Rev. Res. **7**, 023132 (2025).
28. J. Wiersig, Phys. Rev. Res. **5**, 033042 (2023).
29. Y. V. Fyodorov and H.-J. Sommers, J. Math. Phys. **38**, 1918 (1997).
30. A. Welters, SIAM J. Matrix Anal. Appl. **32**, 1 (2011).
31. C. Wang, W. R. Sweeney, A. D. Stone, *et al.*, Science **373**, 1261 (2021).
32. H. Hodaei, A. U. Hassan, S. Wittek, *et al.*, Nature **548**, 187 (2017).
33. A. D. Rakić, A. B. Djurišić, J. M. Elazar, *et al.*, Appl. Opt. **37**, 5271 (1998).
34. C. F. Bohren and D. R. Huffman, *Absorption and Scattering of Light by Small Particles* (John Wiley & Sons, 2008).
35. K. Wang, Q. J. Wang, M. R. Foreman, *et al.*, "Topological engineering of high-order exceptional points through transformation optics," Laser Photonics Rev., https://onlinelibrary.wiley.com/doi/10.1002/lpor.202500593.